

Characteristics of the Grain-Size Composition of Deep-Water Oceanic Sediments

V. N. Sval'nov and T. N. Alekseeva

Shirshov Institute of Oceanology, Russian Academy of Sciences, Nakhimovskii pr. 36, Moscow, 117997 Russia

e-mail: tania@blackout.ru

Received June 21, 2004

Abstract—The grain-size composition of nonlithified sediments in the Indian, Pacific, and Atlantic oceans is studied. Grain-size features of the major lithogenetic types of deep-water sediments are determined. The genetic interpretation of results obtained is given. Trends of the fractionation of sandy-silty and pelitic materials in pelagic zones of sedimentation basins are revealed.

DOI: 10.1134/S0024490206030011

Relationship of size fractions in deep-water oceanic sediments controls three (circumcontinental, latitudinal, and vertical) types of the zonality of natural processes and azonal factors (tectonics, volcanism, hydrodynamics, and gravity). Interaction of processes mentioned above in specific facies settings is reflected in diverse grain-size features of sediments. The aim of the present communication is to reveal certain trends in the initial material fractionation in oceanic pelagic zones based on grain-size parameters of the major lithogenetic types of deep-water sediments.

MATERIALS AND METHODS

We discuss results of the investigation of approximately 3000 samples of nonlithified sediments taken in different periods by authors of the present communication and other researchers of the Shirshov Institute of Oceanology in the Indian, Pacific, and Atlantic oceans (Fig. 1). The wet sieving (grain-size distribution) analysis was carried out by the traditional (Petelin, 1967) and refined Petelin (Alekseeva and Sval'nov, 2000) methods. Some samples were analyzed by the Atterberg method (Tucker, 1988).

The grain-size spectrum of components in the studied samples ranges from $<1\ \mu\text{m}$ to gravel and coarser dimensions. Grains larger than 1 mm are often represented by biogenic remains (detritus and intact shells), which usually preserve the lifetime position in thanatocenosis, authigenic concretions of different compositions, and exotic clasts. Therefore, the sum of $<1\text{-mm}$ fractions was recalculated to 100%. In certain situations, this approach makes it possible to eliminate the random influence of the benthogene, authigenic, and gravitational factors on the distribution of fine-grained components depending on the hydrodynamic regime. After the recalculation, specific features of the grain-size composition of sediments become more vivid, but

the relationship of $<1\text{-mm}$ fractions is retained. It should be noted that the share of the coarse fraction ($>1\ \text{mm}$) in the studied sediments usually does not exceed 5% and cannot noticeably affect their grain-size parameters.

Based on lithogenetic types of sediments (Sval'nov, 2001), the entire data array is divided into statistical samples and subsamples (Table 1) depending on the composition of admixtures differing from the background (biogenic fragments; edaphogenic, underwater, and subaerial volcanic materials; terrigenous minerals of the sandy-silty dimension; and others). The PC-based calculations of contents were performed for 14 fractions and the results obtained were used to compile bar charts, cyclograms, cumulative curves (CC), empirical distribution fields (EDF), and ternary diagrams. Finally, we calculated the following parameters (Sval'nov and Alekseeva, 2003): median (Md), sorting coefficient (So), and coefficients of the pelitic material differentiation Kd and Kd_1 (relations of the subcolloidal fraction to coarse and medium pelite fractions, respectively). The results obtained show that grain-size coefficients (Md, So, Kd, and Kd_1), EDF, and CC are the statistically most informative characteristics of nonlithified sediments.

PETROGRAPHIC COMPOSITION AND DISTRIBUTION OF SEDIMENTS

Oceanic sediments include terrigenous, biogenic, volcanogenic, cosmogenic, edaphogenic, and authigenic components, relationship between which depends on specific facies environments. Despite genetic diversity of the initial material, the ocean floor is characterized by a relatively small group of major sediment types. However, one can identify several varieties of sediments of mixed type in transitional (gener-

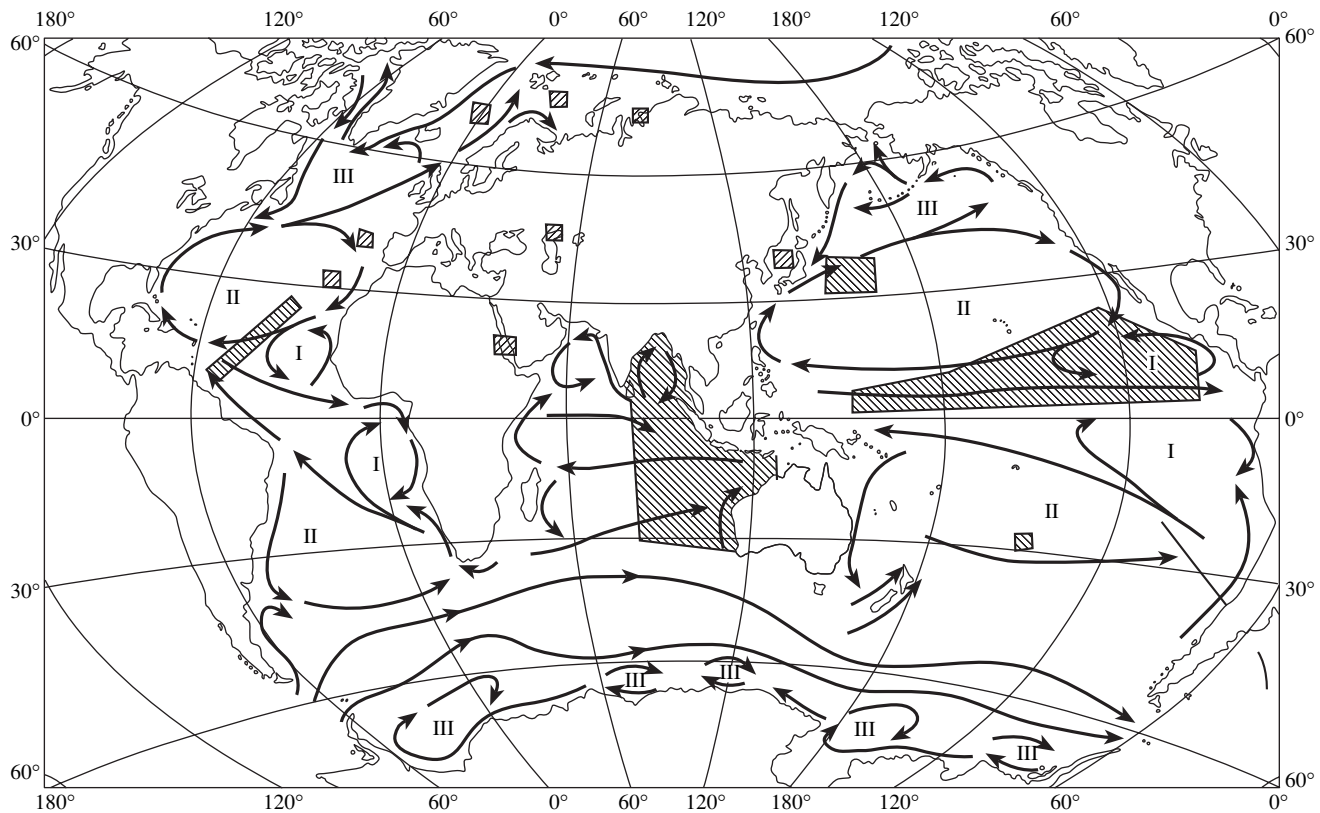


Fig. 1. Location of the studied objects. Major currents on the World Ocean surface (Stepanov, 1974): (I) cyclonic tropic, (II) anti-cyclonic subtropic, (III) cyclonic high-latitude. The studied seafloor areas are shaded.

ally, gradual) zones based on the complex of parameters (Table 1).

Sediments containing more than 70% of the major component are conditionally referred to as one-component ("pure") type. In polycomponent (mixed) sediments, two or more components make up 30–70% each (Murdmaa, 1987). This approach was used for the description of the major types of sediments and their varieties (Sval'nov, 2001).

Clastic sediments include terrigenous, volcanoterrigenous, and volcanoclastic materials with psammitic (sandy) and aleuritic (silty) textures. They are composed of products of the continental rock disintegration or volcanoclastic material (tephra) transported to ocean. Accumulations of edaphogenic material of different grain size fractions (from lumpy slide-rocks to siltstones) consisting from the products of bottom rock disintegration are also included in this group at sediments.

Clayey sediments include pelitic and silty-pelitic varieties with the content of <0.01-mm fraction equal to >70% and 50–70%, respectively. They are mainly composed of genetically different clay minerals and diverse fine-clastic material. The admixture of biogenic, edaphogenic, and authigenic components is noticeable in some places. Clayey sediments are deposited at any depth in the World Ocean, but their composition appre-

ciably changes off the coast. Hemipelagic (including the shallow-water facies), miopelagic, and eupelagic sediments are the major lithofacies types of clays. According to the classification based on the zeolite content (Sval'nov, 2001), the eupelagic clays can be divided into eupelagic sediments (phillipsite up to 30%), zeolite-clayey sediments (phillipsite 30–50%), and zeolitites (zeolite >50%).

Pliocene–Pleistocene eupelagic clays are developed in the central oceanic zones beneath the anticyclonic gyres with low bioproductivity. Such clays are characterized by negligible sedimentation rate, domination of authigenic composition (smectite, phillipsite, palagonite, and ferromanganese nodules), high content of bone detritus, and oxidizing environment.

Sediments of the eupelagic facies give way to Quaternary miopelagic clays at transitions from the anticyclonic gyres to cyclonic gyres with high bioproductivity. The miopelagic clays formed in oxidizing and sub-oxidizing environments have an authigenic terrigenous composition. They are characterized by relatively high sedimentation rate, predominance of terrigenous clay minerals, subordinate role of authigenic formations (micronodules, smectite, celestobarite, and phillipsite), and occasional presence of radiolarians, foraminifers, and other biological components.

Table 1. Statistical samples based on sediment types

Samples	Subsam- ples	Sediment type		Sediment group
1	2	3		4
A. Pliocene-Quaternary sediment				
I (EC)		EC	eupelagic clay	Clayey
		ZC	zeolitic-clayey sediment	
		Z	zeolite	
II (MC)	II a	MC	miopelagic clay	
		rMC	the same (radiolaria-rich)	
		rdMC	the same (radiolaria- and diatom-rich)	
	II b	rlcMC	the same (radiolaria-rich, low-calcareous)	
		lcMC	the same (low-calcareous)	
		rdlcMC	the same (radiolaria- and diatom-rich, low-calcareous)	
II c	trMC	the same (tuffaceous radiolaria-rich)		
III (HC)	III a	HC	hemipelagic clay	
		rHC	the same (radiolaria-rich)	
		dHC	the same (diatom-rich)	
	III b	dlcHC	the same (diatom-rich, low-calcareous)	
		rlcHC	the same (diatom-rich, low-calcareous)	
		rdlcHC	the same (radiolaria- and diatom-rich, low-calcareous)	
		lcHC	the same (low-calcareous)	
	III c	lctHC	the same (low-calcareous tuffaceous)	
		tHC	the same (tuffaceous)	
		dtHC	the same (diatom-rich tuffaceous)	
		rtHC	the same (radiolaria-rich tuffaceous)	
	III d	sHC	the same (silty)	
		SC	silty-clayey mud	
		CS	clayey-silty mud	
		CDS	clayey-diatom-silty mud	
III e	saslcHC	hemipelagic clay with abundant sandy-silty material (low-calcareous)		
	tlcSaSC	sandy-silty-clayey mud (tuffaceous low-calcareous)		
III f	FeHC	hemipelagic clay with Fe (metalliferous)		
IV (R)	IV a	R	radiolarian ooze	
		dR	the same (diatom-rich)	
		DR	diatom-radiolarian ooze	
	IV b	tDR	the same (tuffaceous)	
IV c	lcDR	the same (low-calcareous)		
V (D)	V a	D	diatom ooze	
		rD	the same (radiolaria-rich)	
		CD	clayey-diatom ooze	
	V b	rCD	the same (radiolaria-rich)	
		lcCD	the same (low-calcareous)	
	V c	rtCD	the same (radiolaria-rich tuffaceous)	
V d	CSD	clayey-silty-diatom ooze		
	SCD	silty-clayey-diatom ooze		
VI (CR)	VI a	CR	clayey-radiolarian ooze	
		dCR	the same (diatom-rich)	
Siliceous				

Table 1. (Contd.)

Samples	Subsam- ples	Sediment type		Sediment group
1	2	3		4
VI (CR)	VI b	dlcCR	the same (diatom-rich low-calcareous)	Siliceous
		lcCR	the same (low-calcareous)	
	VI c	lctCR	the same (low-calcareous tuffaceous)	
		tCR	the same (tuffaceous)	
	VI d	FCR	foraminiferal–coccolith–radiolarian ooze	
		CFR	coccolith–foraminiferal–radiolarian ooze	
FR		foraminiferal–radiolarian ooze		
VII (RC)	VII a	RC	radiolarian–clayey ooze	
		dRC	the same (diatom-rich)	
	VII b	lcRC	the same (low-calcareous)	
	VII c	tRC	the same (tuffaceous)	
lctRC		the same (low-calcareous tuffaceous)		
VIII (DC)	VIII a	DC	diatom-clayey ooze	
		RDC	radiolarian–diatom–clayey ooze	
	VIII b	lcDC	diatom–clayey ooze (low-calcareous)	
	VIII c	tDC	the same (tuffaceous)	
		tRDC	radiolarian–diatom–clayey ooze (tuffaceous)	
VIII d	DSC	diatom–silty–clayey ooze		
IX (F)	IX a	F	foraminiferal ooze	
		cF	the same (coccolith-rich)	
		CcF	coccolith-foraminiferal ooze	
		rCcF	the same (radiolaria-rich)	
	IX b	tF	foraminiferal ooze (tuffaceous)	
		tDF	diatom-foraminiferal ooze (tuffaceous)	
		tCcF	coccolith-foraminiferal ooze (tuffaceous with acid volcanoclastics)	
IX c	vCcF	the same (with basic volcanoclastics)		
IX d	pCcF	the same (with pteropods)		
X (C)	X a	Cc	coccolith ooze	Carbonate
		fCc	the same (foraminifer-rich)	
		rCc	the same (radiolaria-rich)	
		FCc	foraminiferal-coccolith ooze	
		rFCc	the same (radiolaria-rich)	
	X b	fvCc	coccolith ooze (foraminifer-rich with basic volcanoclastics)	
		rtCc	the same (radiolaria-rich tuffaceous)	
		tvCc	the same (tuffaceous with basic volcanoclastics)	
		vFCc	foraminiferal–coccolith ooze (with basic volcanoclastics)	
		vSiC	silicate-coccolith ooze (with basic volcanoclastics)	
	X c	sCc	coccolith ooze (silty)	
		fsCc	the same (foraminifer-rich silty)	
sFCc		foraminiferal–coccolith ooze (silty)		
X d	pFCc	the same (with pteropods)		
XI (CIC)	XI a	CIC	clayey–calcareous mud	
		rCIC	the same (radiolaria-rich)	

Table 1. (Contd.)

Samples	Subsam- ples	Sediment type		Sediment group
1	2	3		4
XI (CIC)	XI b	sCIC	the same (silty)	Carbonate
	XI c	MnFeCIC	the same with Mn and Fe (metalliferous)	
XII (CCI)	XII a	CCI	calcareous-clayey mud	
		rCCI	the same (radiolaria-rich)	
		rdCCI	the same (radiolaria- and diatom-rich)	
	XII b	sasCCI	the same (sandy-silty)	
		sastCCI	the same (sandy-silty-tuffaceous)	
	XII c	vCCI	the same (with basic volcanoclastics)	
XII d	FeCCI	the same with Fe (metalliferous)		
	MnFeCCI	the same with Fe and Mn (metalliferous)		
XIII (MD)		MD	mixed detrital sediment	
XIV (CAS)		CoAS	coral-algal sand	
		GSaCoA	gravelly-sandy-coral-algal sediment	
		GCoA	gravelly-coral-algal sediment	
		saGCoA	gravelly-coral-algal sediment (with detrital sand)	
XV (T)		T	acid tephra	Volcaniclastic
		lcT	the same (low-calcareous)	
XVI (VS)		gSaV	volcaniclastic sand (with basic glass and gravel of the same composition)	
		lcSaV	the same (low-calcareous)	
		GSaSV	gravelly-sandy-silty sediment of basic composition	
XVII (MFe)		FeCl	metalliferous (ferruginous-clayey) sediment	Metalliferous
		ClFe	the same (clayey-ferruginous)	
		lcFeMnCl	the same (ferruginous-manganiferous-clayey low-calcareous)	
		lcFeMnCl	the same (manganiferous-ferruginous-clayey low-calcareous)	
		FeMnClC	the same (ferruginous-manganiferous-clayey-calcareous)	
B. Pre-Paleocene sediments				
XVIII (MC)		MCl	miopelagic clay (Miocene)	Clayey
		rMCl	the same (radiolaria-rich)	
		zMCl	the same (zeolite-rich)	
XIX (HCM)		HCIM	hemipelagic clay (Miocene)	Clayey
		rHCIM	the same (radiolaria-rich)	
		sM	silty mudstone	
XX (RS)		RS	radiolarian sediment	Siliceous
		dRS	the same (diatom-rich)	
		CRS	clayey-radiolarian sediment	
		RCS	radiolarian-clayey sediment	
		CRS	coccolith-radiolarian sediment	
XXI (DS)		DS	diatom sediment	Siliceous
		CDS	clayey-diatom sediment	
		DCS	diatom-clayey sediment	
XXII (CS)		CS	coccolith sediment	Carbonate
		rCS	the same (radiolaria-rich)	
XXIII (CFS)		CFS	coccolith-foraminiferal sediment	Carbonate
		cCeRS	the same, clayey sandstone	

Pleistocene and Holocene hemipelagic and shallow-water clays are deposited under conditions of near-continental lithogenesis (high sedimentation rate, reducing environment, and proximity to catchment areas). Such sediments are primarily composed of terrigenous clastic silty and clayey materials with authigenic pyrite, glauconite, rhodochrosite, and biogenic remains (foraminifers, radiolarians, coccolithophorids, and diatoms).

Calcareous sediments. The domain of calcareous sediments is governed by the critical depth of carbonate accumulation (CDC). Above the CDC, calcareous skeletons are well preserved and deposited as monomineral sediments. Below the CDC, the skeletons intensely dissolve and the CaCO_3 content rapidly decreases to the negligible level. The CaCO_3 content is $<10\%$ in noncarbonate sediments. In deep-water zones of the World Ocean, calcareous sediments are mainly represented by the planktonic-foraminiferal, coccolith-foraminiferal, coccolith, foraminiferal-coccolith, and clayey-calcareous varieties. The carbonate sediments include all transitional varieties ranging from pelites to psammites. Pteropod oozes are found in some areas. The benthogenic carbonate sediments are divided into the shelly, foraminiferal, coral-algal, and mixed detrital varieties.

Siliceous sediments. Radiolarians and diatom algae play a crucial role in the formation of siliceous (more correctly, clayey-siliceous) sediments. Based on the prevalence of siliceous skeletons of planktons, the siliceous sediments are divided into the radiolarian and clayey-radiolarian, diatom (including the *Ethmodiscus* and *Thalassiotrix* varieties), clayey-diatom, clayey-*Ethmodiscus*, *Ethmodiscus*-radiolarian, and radiolarian-*Ethmodiscus* oozes. Siliceous-sponge (spicule) oozes are referred to as benthogene sediments.

Calcareous-clayey sediments correspond to pelites (clays) and silty clays. They are mainly composed of fine-clastic and clayey materials (50–70%). The content of fragments of planktonic foraminiferal and coccolith shells is as much as 30–50%. The sediments usually contain an admixture of radiolarians, diatoms, and silt-size clastic minerals (plagioclases, pyroxenes, and others). Radiolarians are present in some places.

Siliceous-clayey sediments are divided into the radiolarian-clayey and *Ethmodiscus*-clayey varieties with siliceous skeletal remains (up to 50%). They correspond to clays and silty clays with respect to grain-size composition. The radiolarian-clayey sediment is composed of clayey and other fine-clastic minerals (50–70%), radiolarian skeletons (30–50%), and a small amount of plagioclases, colorless glass, *Ethmodiscus*, and small diatoms. Low-calcareous radiolarian-clayey oozes are also present.

The *Ethmodiscus*-clayey sediments include clayey and other fine-clastic minerals (50–70%) and *Ethmodiscus* shells (30–50%). The subordinate components are represented by radiolarians, small diatoms, silt-size

allochthonous minerals, and pyrite. The *Ethmodiscus*-clayey sediments are divided into the tuffaceous, low-calcareous, and radiolaria-rich varieties.

Benthogene siliceous-sponge sediments are presumably widespread on the shelf. However, the redeposited variety is found at a depth of as much as 5450 m (Sval'nov, 1983). For example, sediments on the shelf off southern Australia are represented by dark brown dense silty clays with silica microscleres and various spicules (50–70%) and sandy-silty clastic material (30–50%) composed of quartz, feldspars, and glauconite.

The brief petrographic description given above shows that oceanic nonlithified sediments are characterized by a considerable diversity. Therefore, comparison of grain-size parameters can be based on the classification of lithogenetic groups and sediment types in respective statistical samples and subsamples (Table 1).

GRAIN-SIZE COMPOSITION OF SEDIMENTS

Results of the wet sieving method provide insights into the sedimentation setting and lithogenetic types of sediments. Thus, the results obtained serve as a source of genetic information. Table 2 presents average contents of size fractions in statistical samples and subsamples of nonlithified oceanic sediments. The table also gives minimal, maximal, and average values of grain-size coefficients M_d , S_o , K_d , and K_{d_1} . Figure 2 shows the summarized EDF and CC values for sediment groups in different statistical samples.

In terms of essential parameters (relationships of fractions; patterns of EDF, CC, bar charts, cyclograms, and ternary diagrams; M_d , S_o , K_d , and K_{d_1} values; and lithological composition), the oceanic sediments can be divided into two major grain-size types.

Sediments of the first type are dominated by pelitic fractions. The EDF plots are observed as steep curves (incomplete maximums) in the pelitic fraction interval. The CC curves are also similar in this interval. This type includes the deep-water miopelagic and eupelagic clays, calcareous-clayey, clayey-siliceous and siliceous-clayey sediments, metalliferous sediments, shallow-water clays, pre-Pliocene coccolith sediments, and hemipelagic clays (Tables 1, 2; Fig. 2; samples I, II, IV–VIII, XII, and XVII–XXII). Each sample is characterized by specific ranges of grain-size coefficients (M_d , S_o , K_d , and K_{d_1}).

Sediments of the second type include statistical samples III, IX–XI, XIII–XVI, and XXIII (Table 1), i.e., shallow-water clastic sediments of marginal seas, oceanic shelf, deep-water carbonate sediments, Pliocene-Quaternary hemipelagic clays, and volcaniclastic rocks. Pelitic fractions also prevail in some cases (Table 2), but they contain sandy-silty biogenic fragments and genetically different clastic (terrigenous, subaerial volcanic, edaphogenic, and submarine volcanic) components. The respective changes in grain-size

Table 2. Average grain-size characteristics of the major types of sediments in the World Ocean

Subsample	Content of fraction, %											Md, μm	So	Kd	Kd ₁
	fraction, mm								sand	silt	pelite				
	1-0.5	0.5-0.25	0.25-0.1	0.1-0.05	0.05-0.01	0.01-0.005	0.005-0.001	(<0.01)* <0.001							
1	2	3	4	5	6	7	8	9	10	11	12	13	14	15	16
I (EC)															
av	0.07	0.16	0.42	0.31	0.93	14.58	30.87	51.73	0.65	1.24	98.10	4.80	2.0	6.3	1.9
max												7.80	4.9	75.8	5.5
min												2.71	1.6	0.9	1.1
II (MC)															
a	0.02	0.07	0.18	0.16	0.20	14.93	33.43	51.17	0.27	0.36	99.36	4.89	1.9	4.7	1.6
b	0.05	0.08	0.72	1.42	0.79	21.17	32.84	42.69	0.85	2.21	96.93	5.83	2.0	2.2	1.4
c	-	0.03	0.24	1.60	0.80	22.99	32.33	42.02	0.27	2.40	97.34	6.00	2.0	2.5	1.3
av	0.02	0.07	0.20	0.21	0.22	15.16	33.41	50.86	0.29	0.43	99.28	5.57	2.00	3.71	1.43
max												9.75	2.6	28.6	5.0
min												2.91	1.7	0.6	0.8
III (HC)															
a	0.06	0.15	0.78	0.76	2.14	17.99	30.15	42.77	0.99	2.90	96.12	6.01	2.5	2.7	1.5
b	0.16	0.91	2.48	3.20	5.58	17.32	28.16	43.97	3.55	8.78	87.68	5.79	2.4	2.9	1.6
c	0.06	0.13	1.92	3.93	6.30	-	-	87.66	2.11	10.23	87.66				
d	0.41	0.41	3.05	12.36	23.36	10.09	15.84	27.10	3.87	35.72	60.41	36.46	4.2	3.4	1.8
e	0.49	2.69	30.91	16.21	6.43	-	-	43.27	34.09	22.64	43.27				
f	0.45	0.86	2.88	7.96	2.03	-	-	85.81	4.19	10.00	85.81				
av	0.13	0.37	1.79	2.95	5.41	13.71	22.28	34.65	2.29	8.36	89.36	16.09	3.02	3.01	1.64
max												67.57	5.1	15.4	3.3
min												3.73	1.8	1.3	1.0
IV (R)															
a	0.01	0.20	0.60	1.32	1.76	14.32	28.10	54.57	0.81	3.08	96.11	4.50	2.0	4.5	2.1
b	0.02	0.10	1.34	5.23	5.21	17.26	23.97	47.18	1.47	10.44	88.10	6.01	2.5	3.5	2.2
c	0.06	0.40	0.97	1.40	1.94	14.21	27.32	53.47	1.44	3.33	95.23	4.53	2.0	3.9	2.0
av	0.02	0.22	0.73	1.74	2.15	14.90	27.20	52.99	0.97	3.90	95.13	5.01	2.18	3.97	2.07
max												11.61	4.7	11.8	5.7
min												2.85	1.7	0.8	1.2
V (D)															
a	0.04	0.16	0.48	0.65	0.69	16.14	31.44	50.55	0.68	1.33	97.98	4.90	2.0	3.5	1.6
b	0.15	1.32	1.85	1.30	1.42	27.22	35.93	35.93	3.32	2.72	93.96	6.60	2.0	1.4	1.0
c	0.07	0.29	2.41	4.49	1.17	12.95	28.17	50.45	2.77	5.66	91.57	4.93	2.2	4.1	1.8
d	0.09	0.09	2.26	11.72	24.19	12.31	19.42	28.43	2.43	35.92	61.65	15.98	4.1	2.4	1.5
av	0.06	0.33	1.09	2.22	2.88	15.73	29.99	47.91	1.48	5.10	93.41	8.10	2.55	2.81	1.50
max												21.19	4.3	5.6	2.2
min												4.07	1.8	1.0	1.0

Table 2. (Contd.)

1	2	3	4	5	6	7	8	9	10	11	12	13	14	15	16
VI (CR)															
a	0.04	0.21	0.75	1.22	1.55	15.81	31.16	49.70	1.01	2.77	96.23	5.03	2.0	3.5	1.7
b	0.07	0.20	0.81	1.53	1.75	17.19	30.08	48.94	1.07	3.28	95.64	5.10	2.0	3.1	1.7
c	0.03	0.12	2.05	4.80	2.52	16.99	29.09	43.04	2.19	7.32	90.48	5.93	2.3	2.7	1.6
d	0.03	0.45	1.77	2.95	2.94	–	–	91.86	2.26	5.89	91.86				
av	0.04	0.21	0.80	1.37	1.61	16.16	30.87	49.40	1.05	2.98	95.97	5.35	2.12	3.09	1.66
max												8.34	4.4	22.3	5.8
min												2.85	1.7	0.7	1.0
VII (RC)															
a	0.02	0.05	0.30	0.40	0.40	16.78	34.41	47.76	0.37	0.80	98.83	5.27	1.9	3.4	1.4
b	–	0.09	0.47	0.56	0.33	18.05	32.26	48.33	0.56	0.89	98.55	5.18	2.0	2.7	1.5
c	0.03	0.13	1.07	4.58	3.19	–	–	91.01	1.22	7.77	91.01				
av	0.02	0.06	0.33	0.53	0.48	16.92	34.16	47.82	0.41	1.0	98.59	5.23	1.95	3.04	1.48
max												8.44	2.8	7.0	3.3
min												3.47	1.8	0.7	0.8
VIII (DC)															
a	0.20	0.54	1.28	1.51	2.35	20.30	29.31	43.96	2.02	3.86	94.12	6.95	2.4	2.9	1.6
b	0.95	4.42	12.06	8.75	6.89	6.31	27.60	33.02	17.43	15.64	66.93	7.67	5.8	5.2	1.2
c	0.31	0.15	1.46	2.30	0.51	21.64	32.25	41.37	1.92	2.81	95.27	6.06	2.1	2.7	1.3
d	0.05	0.15	1.22	10.63	26.05	12.50	19.22	30.18	1.42	36.68	61.90	16.43	4.2	2.6	1.6
av	0.26	0.54	1.90	3.62	5.65	18.75	28.68	40.05	2.70	9.28	88.02	9.28	3.63	3.33	1.41
max												26.87	5.8	6.0	2.4
min												3.79	1.9	1.0	1.0
IX (F)															
a	2.66	12.34	8.91	7.18	4.95	16.19	21.89	28.20	23.91	12.13	63.97	56.50	6.5	2.5	1.5
b	0.43	1.81	7.10	17.68	21.35	9.98	12.34	21.37	9.34	39.03	51.63	60.10	4.7	2.2	1.7
c	5.80	7.34	5.61	2.44	2.44	14.17	26.99	35.20	18.75	4.88	76.37	50.28	4.1	2.5	1.3
d	35.19	28.17	6.65	4.15	0.75	9.08	3.83	12.19	70.01	4.91	25.09	695.47	4.5	1.3	3.2
av	3.05	11.84	8.67	7.39	5.50	15.68	21.58	28.17	23.56	12.89	63.56	215.59	4.96	2.12	1.92
max												695.47	14.5	12.6	4.2
min												5.51	1.9	0.5	0.5
X (C)															
a	0.94	4.29	5.31	3.91	2.01	18.43	29.57	36.55	10.55	5.92	83.53	7.59	3.0	2.4	1.3
b	3.05	7.60	8.78	4.89	7.21	14.47	27.10	26.52	19.43	12.10	68.47	26.10	4.5	2.4	1.1
c	1.41	3.48	1.23	3.40	0.97	23.97	32.34	33.21	6.11	4.37	89.52	7.27	2.3	1.5	1.0
d	0.77	2.04	2.57	0.53	0.25	31.82	26.49	35.53	5.38	0.78	93.84	7.31	2.5	1.1	1.3
av	1.19	4.62	5.51	3.98	2.54	18.32	29.40	35.21	11.32	6.52	82.16	12.07	3.08	1.87	1.20
max												182.87	11.1	15.4	3.3
min												5.01	1.4	0.5	0.3
XI (CCI)															
a	0.37	2.05	3.11	2.38	1.52	15.20	29.88	46.83	5.52	3.91	90.59	5.66	2.8	3.4	1.6
b	0.18	0.75	1.25	0.60	15.03	–	–	82.18	2.19	15.6	82.18				
c	0.05	0.08	0.47	1.26	0.53	32.00	30.94	36.01	0.60	1.80	97.61	6.86	2.2	1.1	1.2
av	0.35	1.94	2.96	2.31	1.63	15.72	29.92	46.50	5.25	3.94	90.82	6.26	2.52	2.26	1.40
max												14.70	10.6	9.0	2.8
min												3.79	1.5	1.0	0.6

Table 2. (Contd.)

1	2	3	4	5	6	7	8	9	10	11	12	13	14	15	16
XII (CCI)															
a	0.44	1.66	3.28	2.65	3.43	18.98	29.92	46.84	5.37	6.09	88.54	5.51	2.2	2.7	1.6
b	1.55	6.14	35.86	16.40	6.81	–	–	33.24	43.55	23.21	33.24				
c	2.96	9.69	13.12	8.73	5.84	–	–	59.66	25.76	14.58	59.66				
d	0.76	1.82	1.59	1.36	1.00	21.27	26.86	48.05	4.17	2.36	93.47	5.34	2.2	3.0	1.8
av	0.53	1.88	4.16	2.96	3.23	19.31	29.47	47.01	6.57	6.19	87.23	5.42	2.20	2.86	1.71
max												14.82	8.4	8.9	2.7
min												3.67	1.9	1.0	1.0
XIII (MD)															
av	9.50	21.16	27.36	15.08	9.43	–	–	17.47	58.02	24.51	17.47				
XIV (CAS)															
av	30.81	34.72	22.23	4.46	1.72	–	–	6.06	87.76	6.18	6.06				
XV (T)															
av	0.07	0.91	16.00	15.21	6.54	9.05	16.27	28.03	16.99	21.75	61.27	63.13	5.6	3.6	1.8
max												260.89	8.8	10.4	3.1
min												5.62	1.7	1.8	1.0
XVI (VS)															
av	12.76	30.13	9.83	4.80	10.20	9.46	10.09	12.73	52.72	15.00	32.28	367.46	5.4	1.5	1.9
max												851.37	12.2	2.2	3.6
min												65.09	0.7	0.8	0.6
XVII (MFe)															
av	0.19	0.52	1.81	3.21	1.13	26.95	28.30	41.99	2.52	4.34	93.13	6.09	2.2	1.9	1.6
max												7.91	2.5	4.5	3.3
min												4.07	2.0	0.8	1.0
XVIII (MCl)															
av	0.10	0.29	0.81	0.89	1.42	16.79	31.30	59.31	1.20	2.30	96.50	5.27	2.1	3.2	1.6
max												8.74	4.2	8.2	3.7
min												3.37	1.9	1.2	1.0
XIX (HCIM)															
av	0.02	0.09	0.33	1.13	0.78	11.61	33.27	54.56	0.44	1.92	97.65	4.39	1.9	5.2	1.7
max												4.64	2.0	8.7	1.9
min												4.06	1.9	3.5	1.4
XX (RS)															
av	0.01	0.02	0.69	0.77	0.25	16.32	31.42	50.81	0.72	1.02	98.29	4.88	2.0	3.2	1.6
max												5.25	2.0	4.2	1.8
min												4.30	1.9	2.5	1.5
XXI (DS)															
av	–	0.23	0.58	0.69	0.63	–	–	97.87	0.81	1.32	97.87				
XXII (CS)															
av	0.02	0.07	0.33	0.43	1.33	18.40	28.88	50.54	0.42	1.76	97.82	4.91	2.0	2.8	1.8
max												6.19	2.1	3.7	2.9
min												3.79	1.9	1.7	1.3
XXIII (CFS)															
av	0.56	5.95	11.60	8.44	1.29	20.53	23.81	35.19	18.10	9.73	72.16	7.71	3.4	1.7	1.5
max												7.97	3.5	2.0	1.5
min												7.45	3.2	1.5	1.5

Note: * The table presents contents of the sum of <0.01-mm fractions if pelites were not divided into fractions; (–) data absent. See Table 1 for sediment types in statistical samples and subsamples.

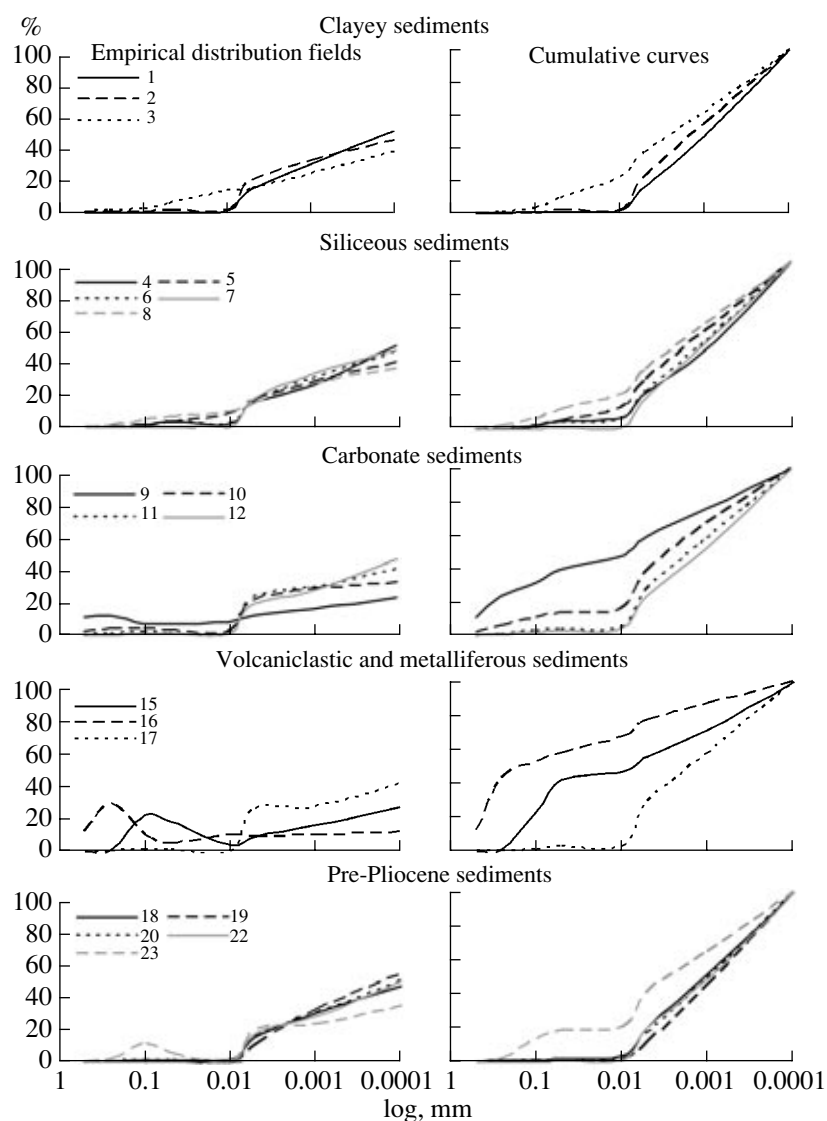


Fig. 2. Average empirical distribution fields and cumulative curves of the major groups of sediments in the World Ocean. See Table 1 for sediment types.

distribution are reflected in bar charts, ternary diagrams, and cyclograms. The EDF values always show relative maximums in the sandy-silty region of the grain-size distribution curve (Fig. 2) and then make up a steep curve with decrease in the pelitic particle size (incomplete maximum). Cumulative curves slowly rise in the sandy-silty part of the grain-size distribution plot and abruptly (or gradually) rise in the pelitic interval.

Sediments of the first and second types also differ in terms of coefficients Md , So , Kd , and Kd_1 (Table 2). It should be noted that the statistical samples can include subsamples with grain-size spectrum differing from that of the averaged sample. For example, sample III (distribution type 2) includes subsamples IIIa, IIb, and IIIf with distribution type 1.

The results obtained indicate that not all grain-size parameters are equally informative for the genetic

interpretation of database. For example, the pelitic material generally predominates in the majority of oceanic sediments (Table 2). Therefore, it is rather difficult to judge about their nature only based on the relationship of fractions. At the same time, the grain-size composition often serves as a reliable basis for the discrimination of lithogenetic types of shallow-water oceanic and marine sediments.

Based on parameters Md and So , one can only identify coarse-grained sediments (sand, silt, tephra, and so on). Their sorting inversely correlates with the Md value. In the finer-grained polygenetic sediments, the Md values are more uniform, but the sorting is better, so, these two parameters are appreciably less informative.

Results of the grain-size analysis can be used for genetic interpretation based on coefficients Kd and Kd_1

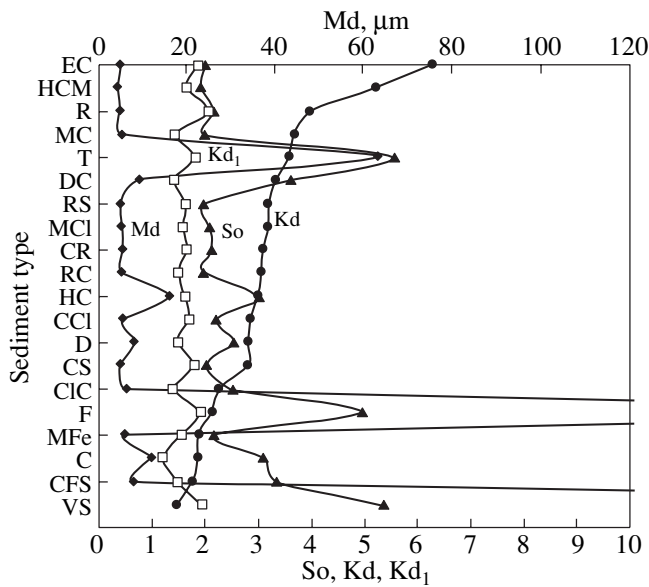


Fig. 3. Average grain-size coefficients (Md, So, Kd, and Kd₁) of the major types of oceanic sediments. See Table 1 for sediment types.

that indicate the differentiation of pelitic material. In general, each sediment type is characterized by a specific Kd value (usually, significantly higher than 1). The Kd value increases toward the basin center (Fig. 3, Table 2). The average Kd₁ value is also always higher than 1, but this parameter is less informative due to the similarity of sizes of medium pelite and subcolloidal particles. Fractionation of the pelitic material is evident from Fig. 4, which shows the dependence of Kd from the sedimentation rate: the share of subcolloidal fraction considerably increases at transition from the hemipelagic facies zone (high sedimentation rate) to the miopelagic and eupelagic (minimal sedimentation rate) zones.

The EDF and CC plots are apparently most important among the results obtained in our work. These plots are particularly useful for the description of subsamples, because they make it possible to discriminate the coarse-grained admixtures that compositionally differ from the background material (biogenic fragments, edaphogenic and volcanic materials, and so on).

The application of bar charts is sometimes useless, because they appreciably mimic the EDF plots. Ternary diagrams and cyclograms are sufficiently informative. Photomicrographs of sediments are obligatory, since they reveal the grain-size distribution.

Thus, results of the grain-size analysis can be used for genetic interpretation if one takes into consideration not only the quantitative characteristics of sediments, but also the shape of plots and specific features of the lithological composition of sediments.

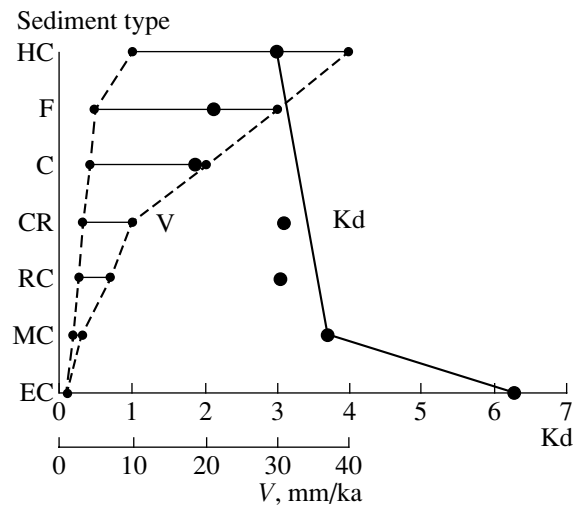


Fig. 4. Sedimentation rate (V) and Kd in pelagic sediments. See Table 1 for sediment types.

GENETIC INTERPRETATION OF RESULTS OF THE GRAIN-SIZE ANALYSIS

The major lithogenetic types of oceanic sediments are confidently distinguished as a result of the explicit prevalence of one component. The grain-size analysis also revealed several transitional varieties (sediments of the mixed type). The grain-size analysis is particularly helpful for the identification of such sediments. In general, the wet sieving analysis should be considered a supplementary method that makes it possible to decipher the genesis of sediments and provides new insights into their lithological composition and sedimentation environment.

Sand, silt, and clay were studied among the terrigenous clastic and clayey sediments. The relatively coarse-grained sediments of marginal seas (Table 2, Fig. 2) are characterized by high Md, So, and Kd values. EDF maximums are distinct in the sandy-silty portion of the grain-size spectrum. Increase in the CC value is gradual at the sand-to-silt transition and is abrupt (or gradual) in finer particles. These features are also typical of volcanoclastic rocks (acid tephra and basaltic sand).

Terrigenous clayey sediments are characterized by good sorting, low Md value (average 5–6 μm), absence of prominent maximums in the EDF plot, and abrupt increase of the CC value in the pelitic fraction of the grain-size spectrum. The Kd and Kd₁ values gradually increase off the coast. However, these parameters (particularly, Kd) are noticeably higher in sediments of marginal seas relative to the oceanic pelagic clays (Sval'nov and Alekseeva, 2003). It should be noted that appreciable variations in the grain-size spectrum can be caused by the admixture of terrigenous, biogenic, and volcanic fragments of the sandy-silty dimension.

Biogenic carbonate sediments (Table 2, Fig. 2) are marked by the medium- and low-grade sorting, highly

variable Md values, and the presence of differently expressed EDF maximums in the sandy-silty portion of the grain-size spectrum. Cumulative curves gradually rise with decrease in particle size. Only the calcareous-clayey and clayey-calcareous sediments show a drastic rise of the CC value in the pelitic interval of grain-size distribution. The average Kd value commonly does not exceed 3, while the Kd_1 value is always less than 2. The presence of alien admixtures (volcaniclastic, terrigenous, and siliceous biogenic fragments) slightly modifies the grain-size spectrum of carbonate sediments.

Biogenic siliceous sediments (Table 2, Fig. 2) are characterized by the good and medium sorting, low Md values (generally, $<10 \mu\text{m}$), and the absence of prominent EDF maximums. One can see small maximums in the sandy-silty region if the sediments contain abundant terrigenous or biogenic carbonate fragments and volcaniclastic material. The cumulative curves are usually steep in the pelitic portion of the grain-size distribution plot. The average Kd value ranges from 3 to 4, while the Kd_1 value varies from 1.5 to 2.1.

Thus, the shape of EDF and CC plots, as well as Md, So, Kd, and Kd_1 values, are most important for the genetic interpretation of results of the grain-size analysis. The presence of alien (relative to the background material) admixtures inevitably affects the grain-size distribution and compels us to analyze specific features of the lithological composition and sedimentation environment of sediments. It should be noted that the impact of authigenic formations (zeolites, micronodules, and so on) is virtually negligible for the grain-size distribution in deep-water sediments.

TRENDS IN THE FRACTIONATION OF SEDIMENTARY MATERIAL IN OCEANS

Relationship of grain-size fractions in sedimentation basins is primarily controlled by the lithodynamics, i.e., processes of transport and fixation of the solid sedimentary material (sediment particles or mass) on the seafloor. All displacements of such material are subdivided into the vertical (sedimentation) and lateral (subparallel to the seafloor) flows (Murdmaa, 1987). Transitional flows include the jumpwise transformation and other motions.

In vertical sedimentation flows, material with negative buoyancy settles according to the particle-by-particle mechanism or as a result of the biofiltrational pelletal transport (Honjo, 1976, 1977). Thus, the sediments are continuously accumulated to form pelagic sediments in central sectors of basins or on flat summits of large rises if the water current is weak. Under other conditions, the sediments are intensely redistributed by hydrodynamic and gravitational flows. According to some researchers, sedimentation flows also produce the so-called "nepheloidites", i.e., nepheloid layers related to bottom currents, avalanches, gravitation flows, bioturbation, decomposition of faecal pellets (Honjo,

1976), discharge of muddy river waters, and so on (Murdmaa, 1987). Such sediments are rather widespread in near-continental areas of basins (Hollister et al., 1972; Murdmaa and Mikhina, 1979) characterized by the contrast distribution of sedimentary material.

In lateral near-bottom hydrodynamic flows, the water volume always prevails over the solid phase volume and they constantly interact with seafloor surface to exchange energy and matter. Sediments of hydrodynamic flows can be divided into two lithodynamic types: bottom currents ("currentites") and contourites (Murdmaa, 1987). Under the influence of intertidal and quasistationary bottom currents, accumulative aprons are formed near the foothills of positive morphologies owing to the washout of fine-grained material from the summit. In some places (e.g., the Samoa Pass), flanks of abyssal valleys incorporate sandy bars behind large ridges of bedrocks or boulder accumulations elongated along the current (Hollister et al., 1974; Leont'ev, 1987). Bottom currents not only produce accumulative aprons, but also constantly transport and redistribute the sedimentary material over the vast spaces of deep-water basins. In contrast to "currentites," the contourites are related to the erosion, transport, and deposition of terrigenous material by deep-water bottom currents parallel to bathymetric contours of the continental foothill (Heezen et al., 1966).

Submarine storms (Hollister et al., 1984) that appear approximately once in two months are an essential hydrodynamic factor of the lateral transport of solid material. When passing from the Polar region to equator, the deep cold waters deviate to west under the influence of the Coriolis force and lean to the western margins of oceans and western slopes of seamounts. This effect is responsible for increase in the velocity of currents. Superposition of influences of the deep-water current and submarine storm (vortex) fosters the erosion of seafloor. Consequently, the currents transport and redeposit the turbid sediment. At the same time, the weaker but stable currents can entrain the turbid matter over great distances.

According to (Murdmaa, 1987), gravitational sediments (gravitites) include the submarine avalanche, landslide, and debris (hereafter, submarine talus), as well as deposits related to the creep and flow of sedimentary material (hereafter, turbid material). Gravitites are widespread near the continent, but they also occur in pelagic zones. As a result of the transformation of autokinetic flows in the course of transportation, gravitational sediments can make up a continuous series ranging from the slip monoliths to submarine landslides and turbidites that are similar to both gravitites and hydrodynamic deposits (Fisher, 1983). Pelagic zones are characterized by unsorted accumulations of basaltic rubble near the foothill of steep slopes within mid-oceanic ridges and transform faults. Edaphogenic talus (gruss-rubble) deposited on slopes of seamounts and strike-slip depressions occasionally contain a sig-

nificant admixture of the fine-grained pelagic material (Murdmaa, 1987; Sval'nov, 1983). Genetically different turbidites are also common here (Sval'nov, 1991).

The brief description of the major lithodynamic types of marine and oceanic sediments presented above testify to an intricate interaction of various factors and mechanisms of sedimentary matter distribution on the sedimentation basin floor. These interactions ultimately develop the grain-size composition of sediments. Without taking the polygenetic coarse-clastic sediments into consideration, we can affirm that the relationship of size fractions in sandy-clayey sediments is primarily governed by hydrodynamic and gravitational processes. Bottom currents control the lateral transport and fractionation of sedimentary material, while gravitational forces provide its subvertical settling on the seafloor.

Lateral sediment flows in the pure form appear only in the coastal zone. They make up coarse-clastic and coarse-grained deposits by the mechanism of saltation and traction along the seafloor. The fine-grained turbid material is transported off the coast and left in the suspended state for a long time. Aerosols (terrigenous, subaerial volcanogenic, and technogenic materials), dead organisms, and products of their vital activity settle on the seafloor by the mechanism of particle-by-particle settling or biofiltrational pelletal transport. In the course of settling on the seafloor, the sediments are subject to the influence of surface, deep, and near-bottom currents. Deviation of particulates from the vertical trajectory has negative correlation with their size and positive correlation with depth.

The existence period of particulates in the suspended state also depends on the presence of frontal, divergent, and convergent zones in the halistase water structure (Stepanov, 1974). In particular, the settling of suspension is evidently accelerated in convergent zones and decelerated in divergent zones.

Mechanical differentiation of material—the major form of lateral flows (hydrodynamic processes)—fosters the grading of coarse-grained sediments into fine-grained varieties with increasing distance from the coast (circumcontinental zonality). Pelitic particles also obey this rule. Vertical sedimentation flows (gravitational processes) primarily generate tephroids and biogenic sediments. The grain-size composition of the biogenic sediments depends on the bioproductivity of surface waters (latitudinal zonality) and the response of skeletal remains to processes of dissolution (vertical zonality).

Thus, the great diversity of grain-size characteristics of oceanic sediments is related to the interaction of hydrodynamic and gravitational processes. The terrigenous (fluviogenic) material is mainly fractionated by currents, whereas the biogenic and aerosol components passively settle on the seafloor. Superposition of these components on the terrigenous material occasionally shifts the grain-size spectrum toward the coarser frac-

tions. Coarsening of sediments in some places is related to the activity of various gravitational flows (including the turbid ones) and the dispersion of edaphogenic material by bottom currents in tectonically active zones.

CONCLUSIONS

Hydrodynamics (mobilization and lateral transport of primary material) and gravitation (settling of terrigenous, biogenic, subaerial volcanogenic, and technogenic components) are the major processes responsible for the grain-size distribution. In shelf zones of the World Ocean and marginal seas, the grain-size composition is controlled by the circumcontinental zonality of natural processes according to the law of mechanical differentiation of material. The relationship of fractions in deep-water sediments is influenced by the latitudinal and vertical zonality of bios distribution, as well as azonal phenomena, such as tectonics, volcanism, bottom currents, and gravity-related slope processes.

Based on characteristic properties, all of the studied lithogenetic varieties of sediments correspond to two major types of grain-size spectrum. The first type includes the deep-water miopelagic and eupelagic clays, calcareous-clayey, clayey-siliceous, and siliceous-clayey sediments, metalliferous sediments, and pre-Pliocene coccolith sediments and hemipelagic clays. The second type includes the shallow-water clastic sediments of marginal seas and oceanic shelf, deep-water carbonate sediments, Pliocene-Quaternary hemipelagic clays, and volcanoclastic sediments.

The pelitic material is subject to mechanical differentiation at any depth. The degree of fractionation of such material is indicated by dimensionless coefficients K_d (the ratio of subcolloidal particles to coarse pelite) and K_{d1} (the ratio of subcolloidal particles to medium pelite). Values of these parameters increase toward the basin center. Biofiltrators only accelerate the settling of fine material (pelletal transport), but they do not affect its distribution on the seafloor where the relationship of pelitic fractions in suspension is inherited passively.

The methodical approach based on the lithogenetic type of sediments makes it possible to obtain grain-size characteristics of samples and determine the genesis of sediments on the basis of grain-size parameters. Thus, the proposed method provides the solution of both direct and inverse problems. We believe that the advantage mentioned above is very essential for complex geological investigations.

REFERENCES

- Alekseeva, T.N. and Sval'nov, V.N., Techniques for Grain Size Analysis of Fine-Grained Sediments, *Okeanologiya*, 2000, vol. 40, no. 2, pp. 304–312 [*Oceanology* (Engl. Transl.), 2000, vol. 40, no. 2, pp. 281–288].
- Fisher, R.V., Flow Transformations in Sediment Gravity Flows, *Geology*, 1983, vol. 11, no. 5, pp. 273–274.

- Heezen, B.C., Hollister, C.D., and Ruddiman, W.F., Shaping of the Continental Rise by Deep Geostrophic Contour Current, *Science*, 1966, vol. 152, no. 3721, pp. 520–528.
- Hollister, C.D., Ewing, M., Heezen, B.C., et al., *Initial Reports of the DSDP*, Washington: US Gov. Print. Off., 1972, vol. 11.
- Hollister, C.D., Johnson, D.A., and Lonsdale, P.F., Current Controlled Abyssal Sedimentation: Samoan Passage, Equatorial West Pacific, *J. Geol.*, 1974, vol. 82, no. 3, pp. 275–300.
- Honjo, S., Coccoliths: Production, Transportation and Sedimentation, *Mar. Micropaleontol.*, 1976, vol. 1, pp. 65–79.
- Honjo, S., Biogenic Carbonate Particles in the Ocean: Do They Dissolve in the Water Column? in *The Fate of Fossil Fuel CO₂ in the Ocean*, London: Plenum Press, 1977, no. 4, pp. 269–294.
- Hollister, C.D., Nauell, A.R., and Jumars, P.A., Restless Depths, in *The World of Science*, 1984, no. 5, pp. 4–16.
- Leont'ev, O.K., Abyssal Bottom Currents as a Geomorphologic Factor, *Geomorfologiya*, 1987, no. 1, pp. 3–16.
- Murdmay, I.O., *Fatsii okeanov* (Oceanic Facies), Moscow: Nauka, 1987.
- Murdmay, I.O. and Mikhina, V.V., Lithology of Sedimentary and Volcanosedimentary Rocks, in *Geologicheskie formatsii severo-zapadnoi chasti Atlanticheskogo okeana* (Geological Rock Associations of the Northwestern Atlantic Ocean), Moscow: Nauka, 1979, pp. 32–66.
- Petelin, V.P., *Granulometricheskii analiz donnykh osadkov* (Grain Size Distribution Analysis of Bottom Sediments), Moscow: Nauka, 1967.
- Stepanov, V.N., *Mirovoi okean: Dinamika i svoistva vod* (The World Ocean: Water Dynamics and Properties), Moscow: Znaniye, 1974.
- Sval'nov, V.N., *Chetvertichnoe osadkoobrazovanie v vostochnoi chasti Indijskogo okeana* (Quaternary Sedimentation in the Eastern Pacific Ocean), Moscow: Nauka, 1983.
- Sval'nov, V.N., *Dinamika pelagicheskogo litogeneza* (Dynamics of Pelagic Lithogenesis), Moscow: Nauka, 1991.
- Sval'nov, V.N., *Mikrostruktury i tekstury glubokovodnykh osadkov* (Microstructures and Textures of Pelagic Sediments), Moscow: GEOS, 2001.
- Sval'nov, V.N. and Alekseeva, T.N., Differentiation of Pelitic Material in Sedimentation Basins, in *Geologiya morei i okeanov* (Geology of Seas and Oceans), Moscow: GEOS, 2003, vol. 2, pp. 100–101.
- Tucker, M., *Techniques in Sedimentology*, New York: Blackwell, 1988.